Electronic Supplementary Material (ESI) for Journal of Materials Chemistry A.
This journal is © The Royal Society of Chemistry 2022

Supporting Information

Clarification of Li Deposition Behavior on Anodes with a Porous Interlayer in Li-free All-Solid-State Batteries

Se Hwan Park†, Dayoung Jun†, Ji Eun Jung, Seong Gyu Lee, Gyu Hyun Lee, and Yun Jung Lee*

Department of Energy Engineering, Hanyang University, Seoul 04763, Republic of Korea

Correspondence: yjlee94@hanyang.ac.kr

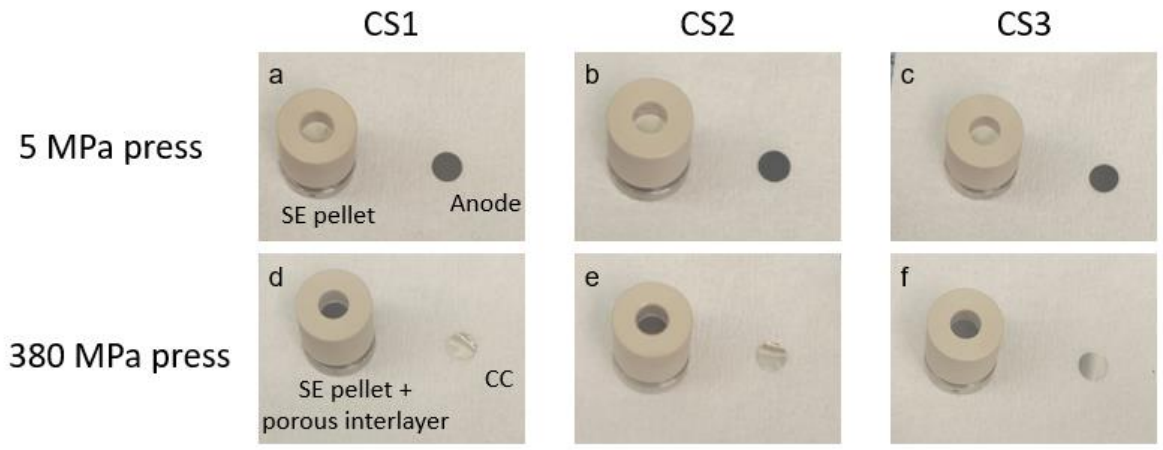

Fig. S1 Photographs of peel-off tests of the anode−SE pellet assembly after forming the SE−porous layer interfacial contact at a pressure of 5 (a, b, and c) and 380 MPa (d, e, and f). The anode was detached by sticky tape. The SE pellet (or SE pellet + porous interlayer) and anode (or CC) were shown in the left and right side of each photograph.

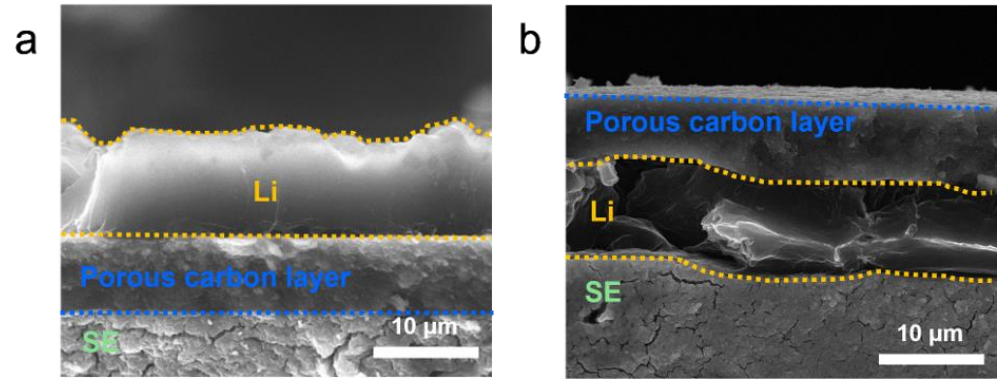

Fig. S2 Cross-sectional SEM images of a Li deposited composite anode when the interfacial contact between the porous interlayer and SE was formed at (a) 380 MPa and (b) 5 MPa. Li was plated at a current density of 0.5 mA cm^{-2} to a capacity of 3 mAh cm^{-2}.

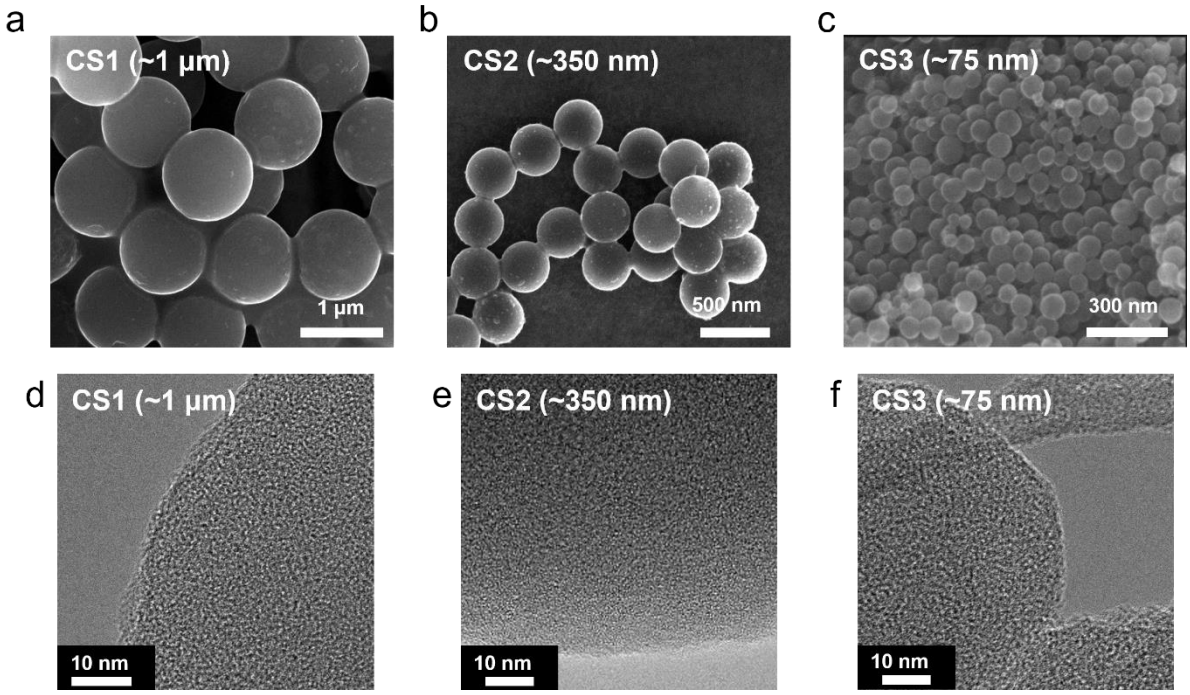

Fig. S3 (a–c) SEM images and (d–f) high-resolution TEM images of (a and d) CS1, (b and e) CS2, and (c and f) CS3.

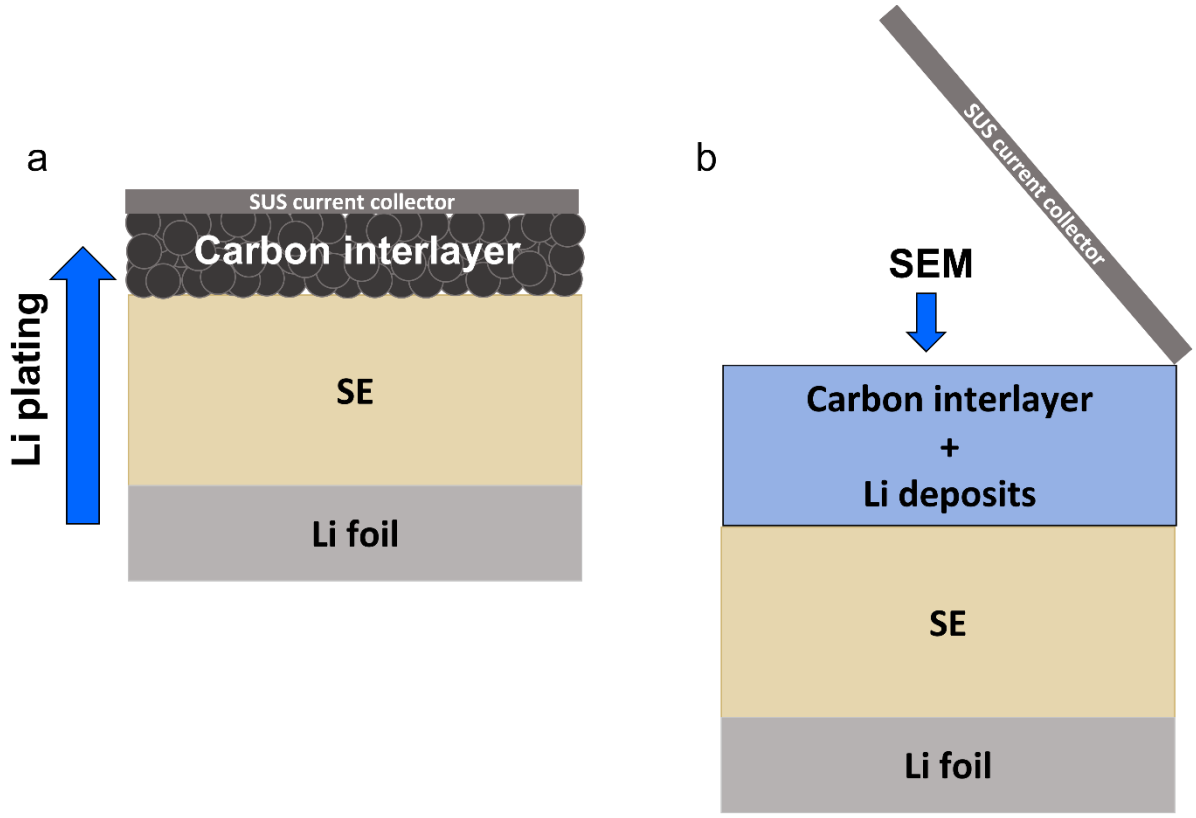

Fig. S4 (a) Schematic illustration of the Li plating of anodes with a carbon-based composite. (b) Schematic illustration of the top-view SEM observation after Li plating and removing the SUS current collector.

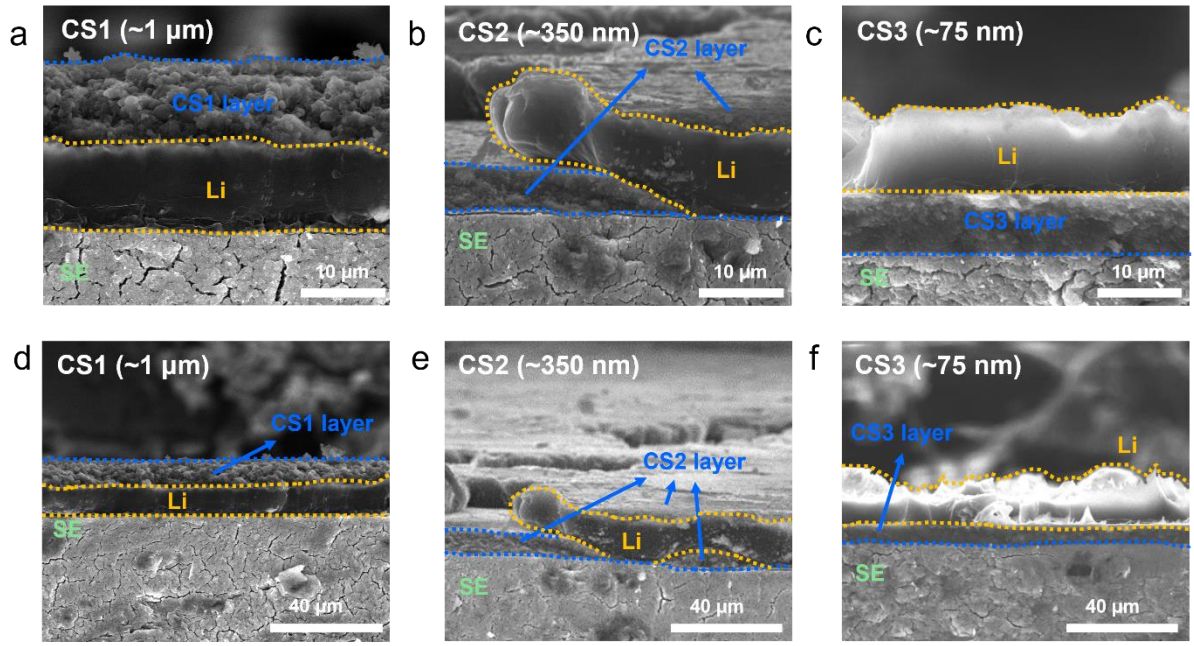

Fig. S5 Cross-sectional SEM images of Li deposited composite anodes plated to 3 mAh cm^{-2} with the boundaries marked for clear distinction: (a and d) CS1, (b and e) CS2, and (c and f) CS3.

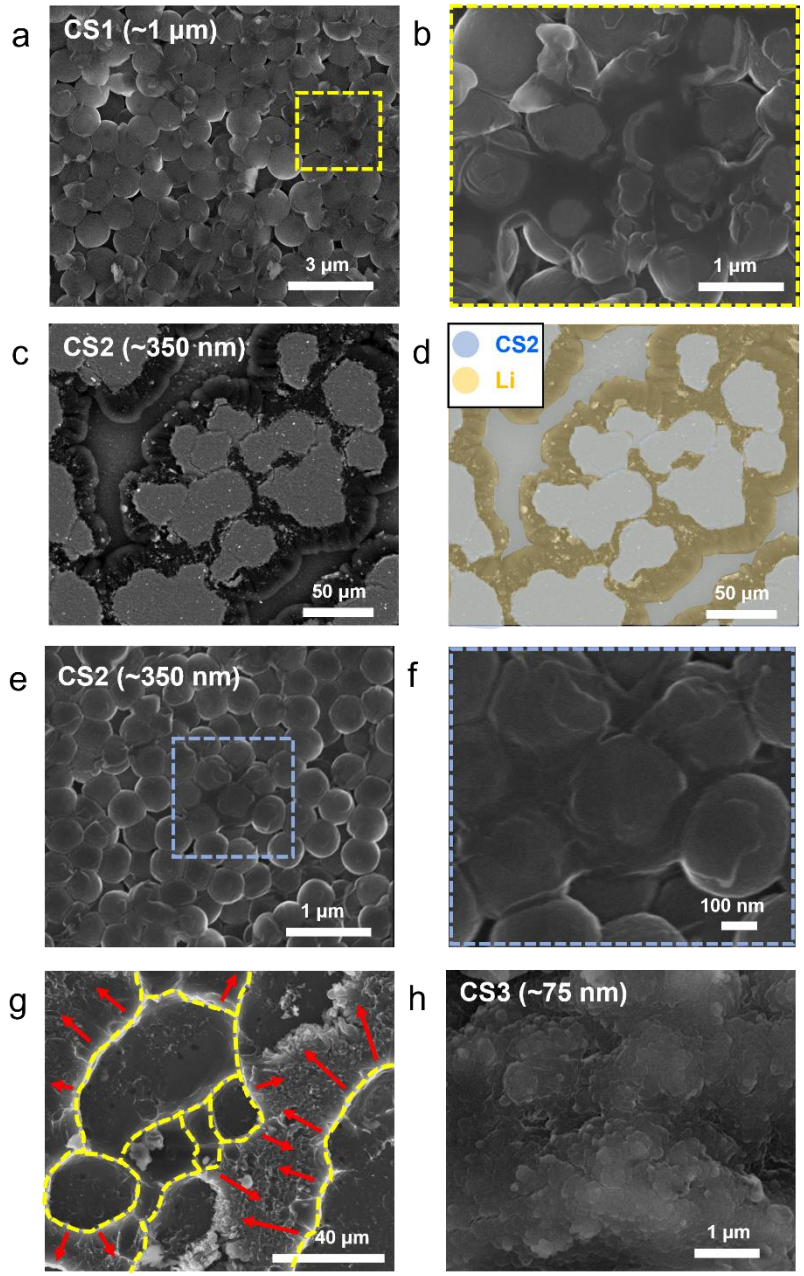

Fig. S6 Additional SEM images after Li plating to a capacity of 3 mAh cm^{-2}. (a–f) Top-view SEM images after Li deposition at 3 mAh cm^{-2}. (a) CS1 and (b) enlarged image of the yellow square in Figure S5a where Li filled the voids. (c) Backscattered electron (BSE) mode SEM images and (d) a colored image of Figure 2e for the Li deposited CS2 composite anode. (e) CS2 layer and (f) enlarged image of blue square in Figure S5e where Li filled the voids. (g) SEM images of the Li deposited CS3 composite anode (Figure 2f) with the boundary lines marked. (h) Cross-sectional SEM image of the CS3 layer after Li deposition at 3 mAh cm^{-2}.

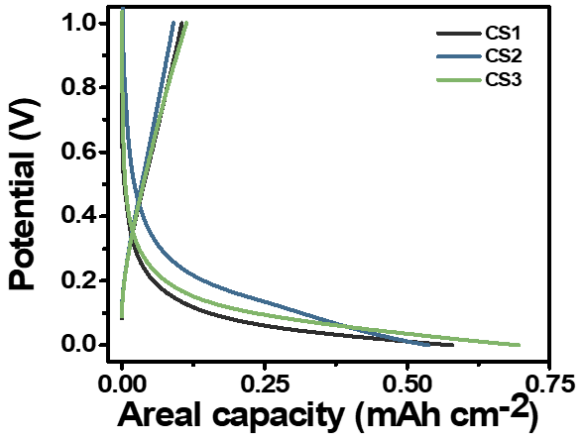

Fig. S7 Voltage profiles of CS1, CS2, and CS3 composite anodes during the initial activation cycle prior to Li deposition.

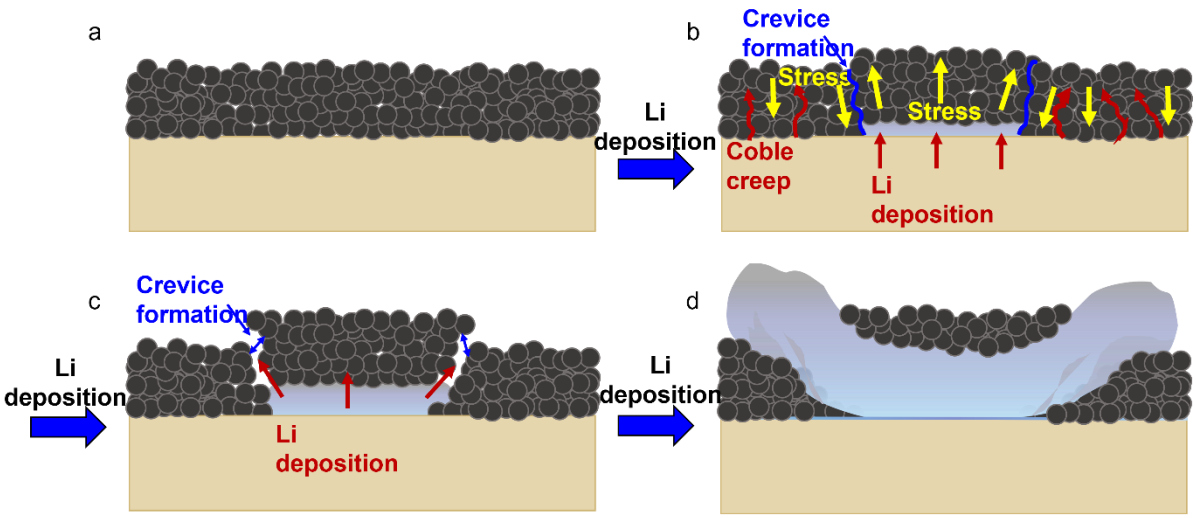

Fig. S8 Proposed scenario for the Li deposition process on the CS2 composite anode.

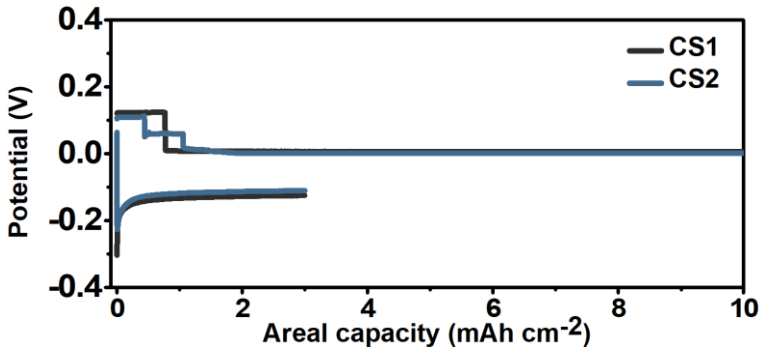

Fig. S9 Voltage profile of CS1and CS2 composite anodes when short-circuiting occurs.

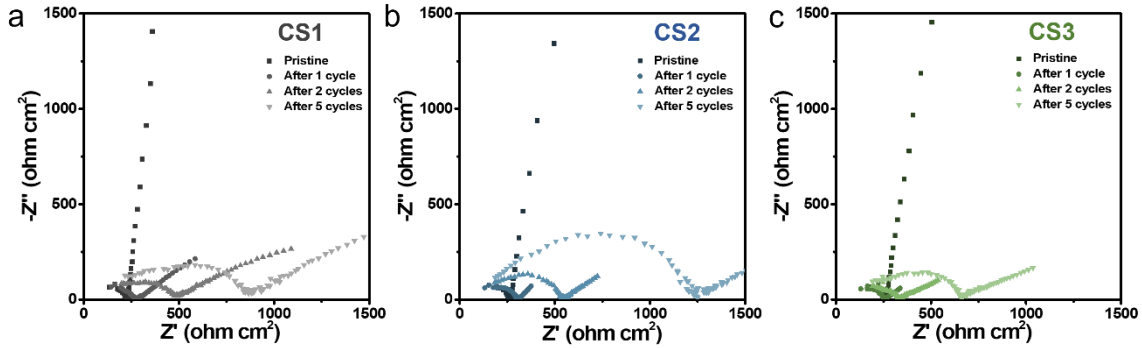

Fig. S10 Electrochemical impedance spectroscopic (EIS) analysis for (a) CS1, (b) CS2, and (c) CS3 in a pristine state (before testing) and after repeated Li plating and stripping.

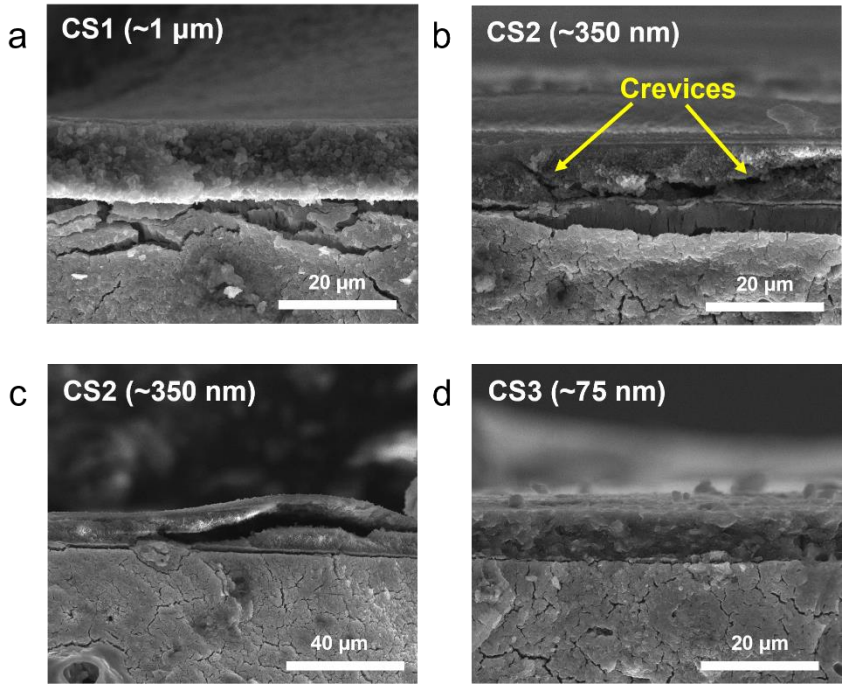

Fig. S11 Cross-sectional SEM images of composite anodes after Li deposition to 3 mAh cm^{-2} and stripping to 1 V at a current density of 0.5 mA cm^{-2}. (a) CS1, (b and c) CS2, and (d) CS3.

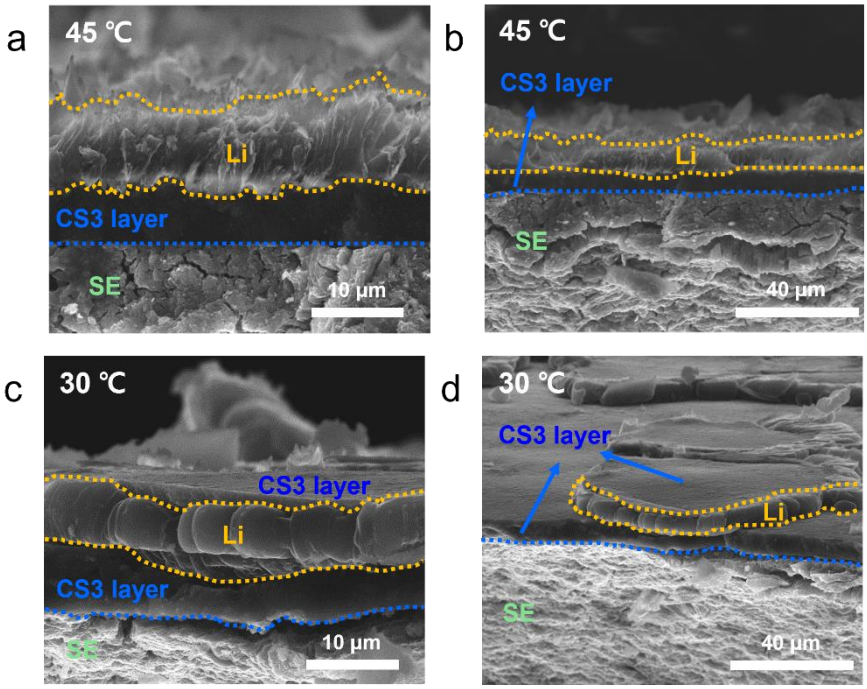

Fig. S12 Cross-sectional SEM images of the Li deposited composite anode plated to 3 mAh cm^{-2} at (a and b) 45 ℃ and (c and d) 30 ℃. The boundaries are marked for clarity.

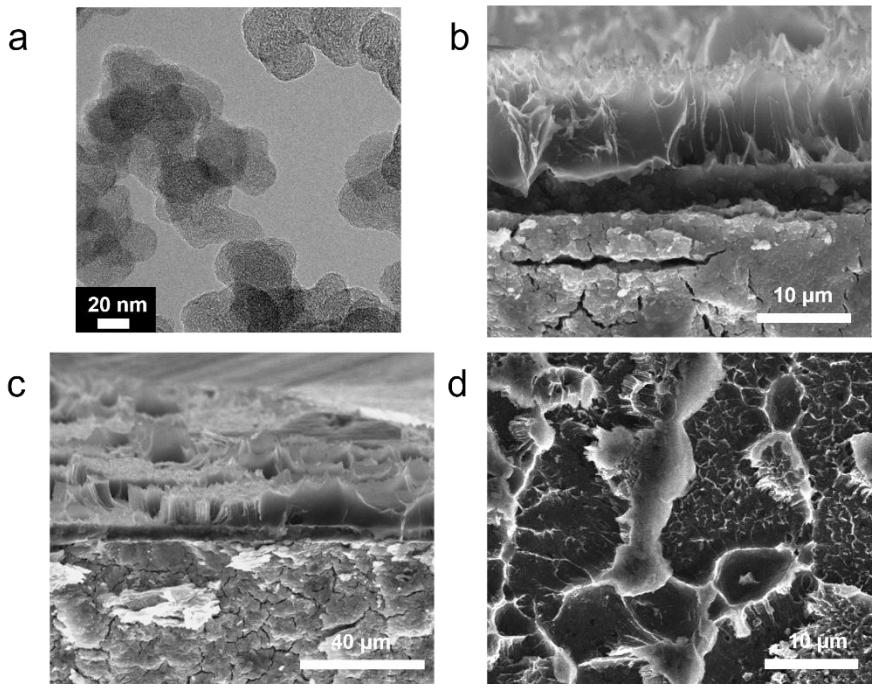

Fig. S13 (a) TEM images of commercial carbon black (SC65). (b and c) Cross-sectional and (d) top-view SEM images of the Li deposited SC65 composite anode plated to a capacity of 3 mAh cm^{-2}.

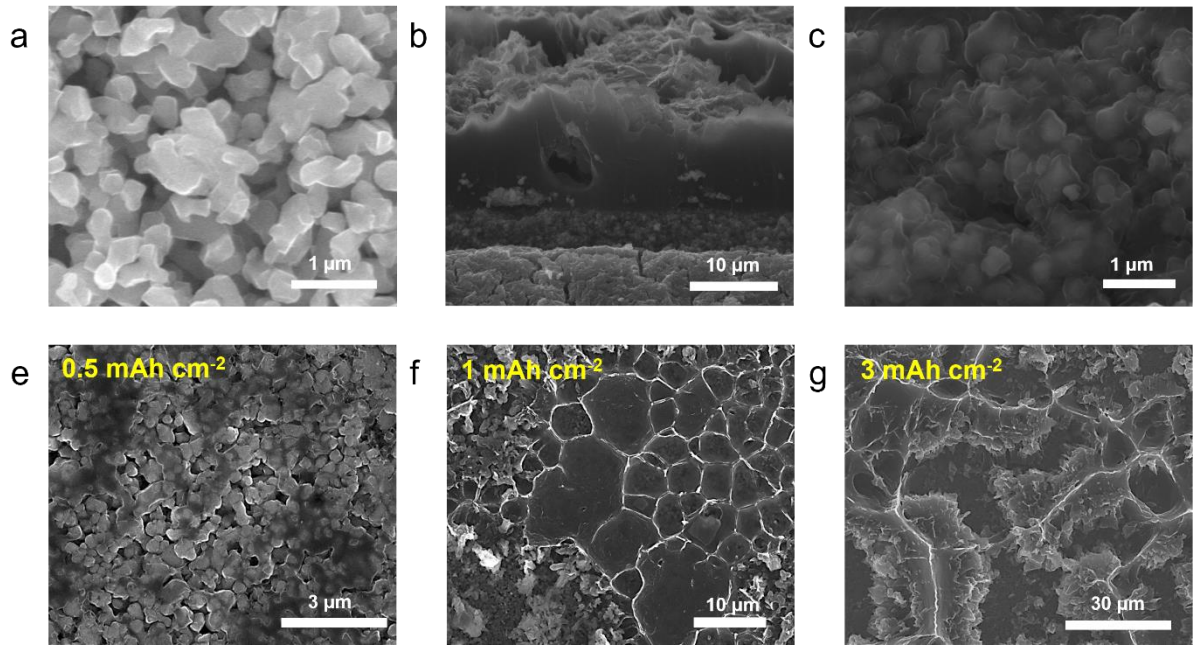

Fig. S14 (a) SEM image of LTO used in the composite anode. (b) Cross-sectional SEM images of the Li deposited LTO composite anode and (c) a magnified image of the LTO layer. (e−f) Top-view SEM images of the Li deposited LTO composite anode with Li plated at capacities (e) 0.5, (f) 1, and (g) 3 mAh cm^{-2}.

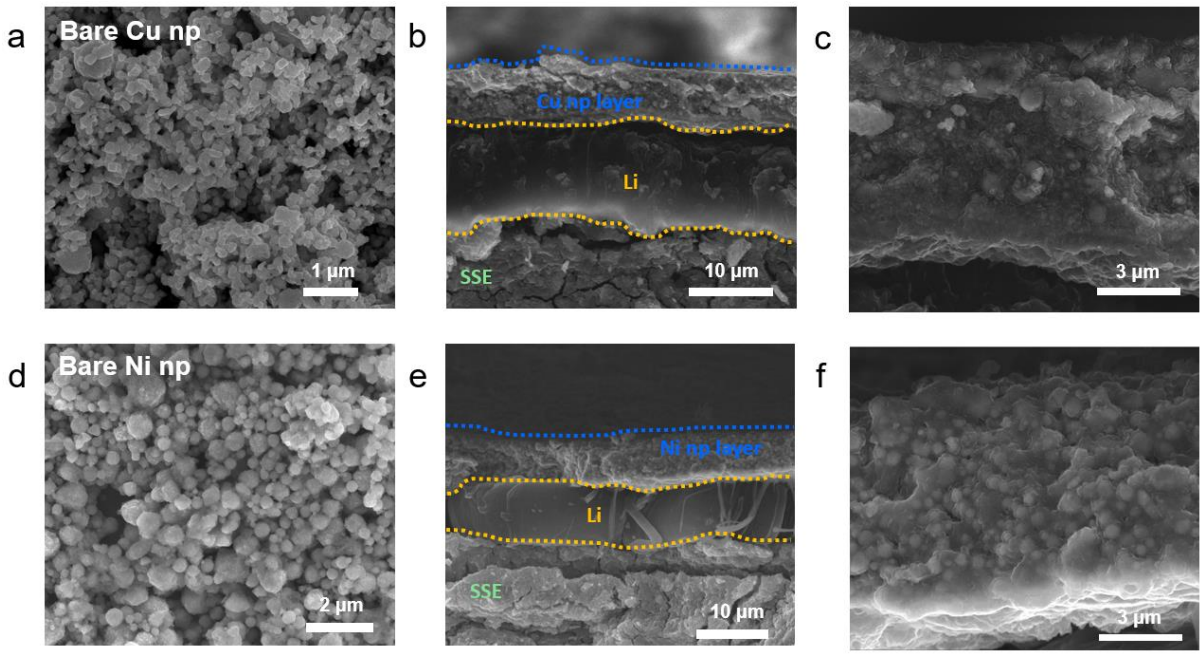

Fig. S15 SEM image of (a) Cu and (d) Ni nanoparticles used in composite anode. Cross-sectional SEM images of Li deposited (b) Cu and (e) Ni composite anode plated to the capacity of 3 mAh cm^{-2}. Enlarged SEM images of (c) Cu and (f) Ni interlayer.

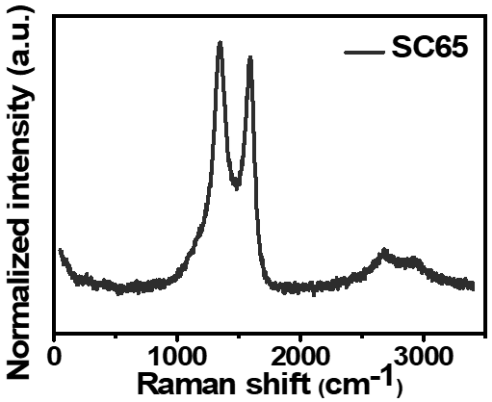

Fig. S16 Raman spectra of SC65 carbon.

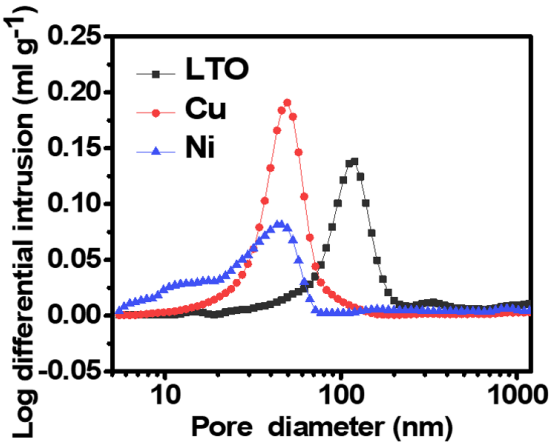

Fig. S17 Pore size distribution of LTO, Cu, and Ni electrodes obtained by mercury porosimetry.

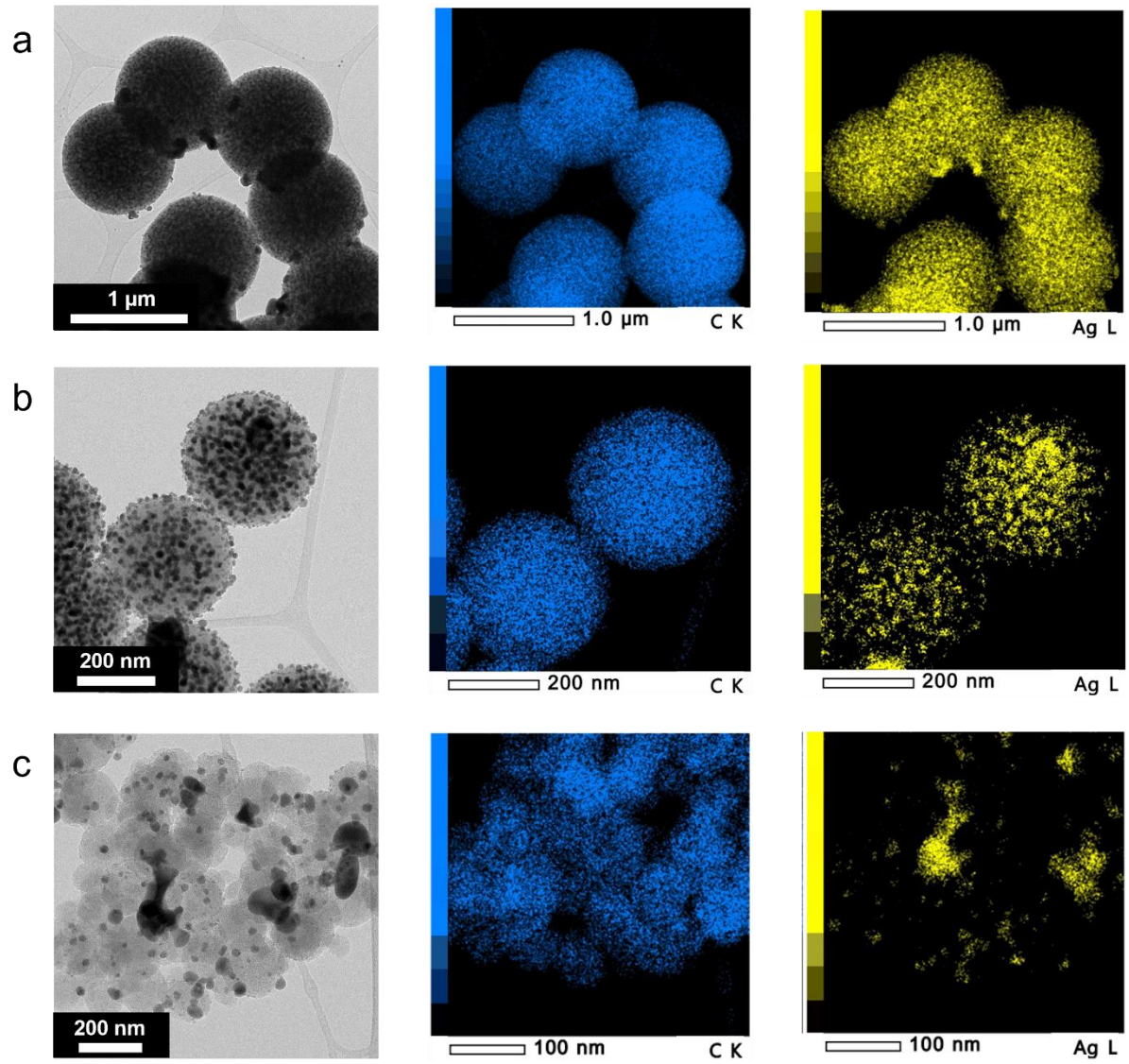

Fig. S18 TEM images and corresponding EDS elemental maps for (a) Ag-CS1, (b) Ag-CS2, and (c) Ag-CS3.

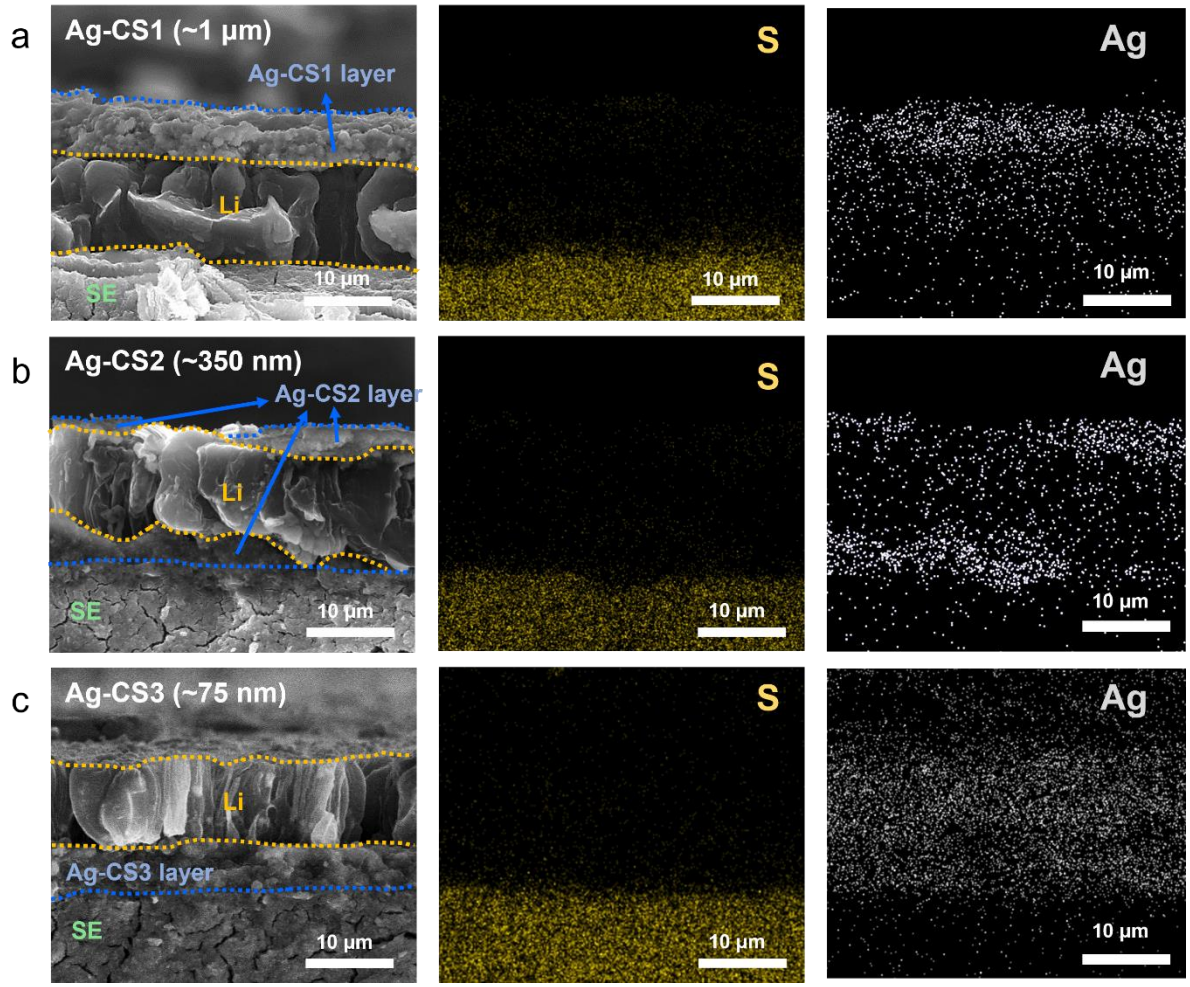

Fig. S19 Cross-sectional SEM images with boundaries marked and corresponding EDS mapping images for Ag-CS composite anodes with Li plated to a capacity of 3 mAh cm^{-2}: (a) Ag-CS1, (b) Ag-CS2, and (c) Ag-CS3.

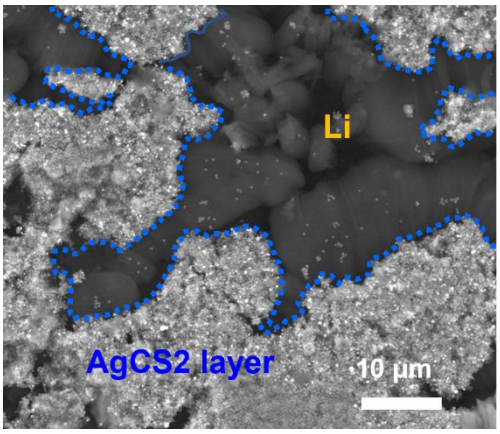

Fig. S20 BSE-mode SEM image of Figure 6h (top-view SEM image of the Ag-CS2 composite anode after Li deposition at 3 mAh cm^{-2})

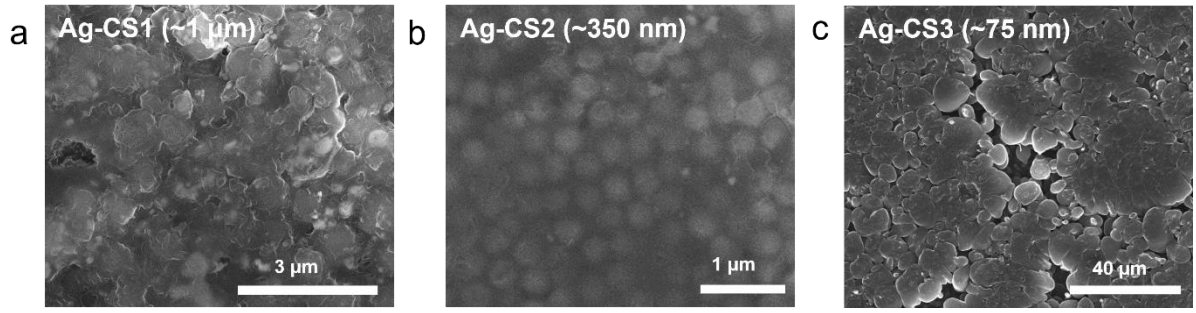

Fig. S21 Top-view SEM images after Li deposition at 3 mAh cm^{-2} for (a) Ag-CS1, (b) Ag-CS2, and (c) Ag-CS3.

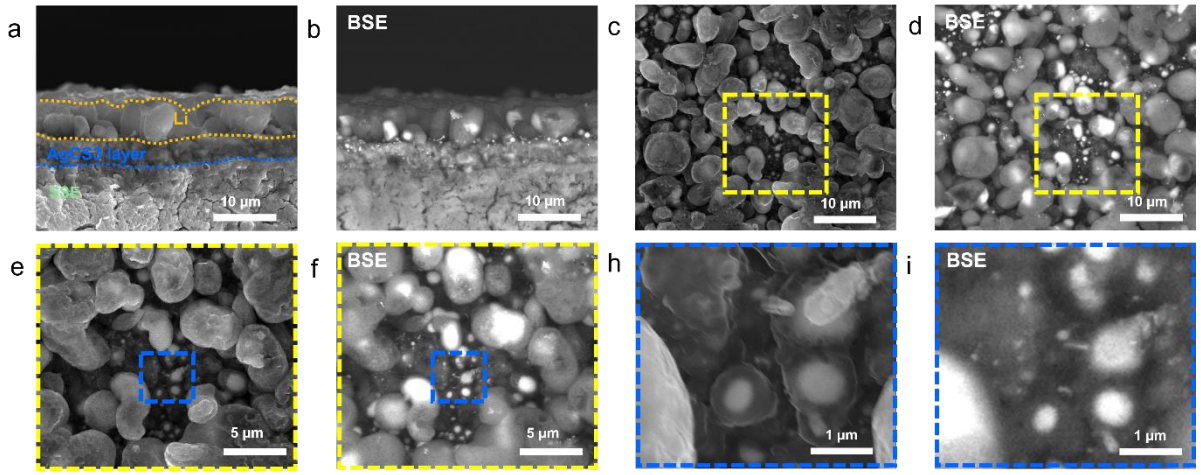

Fig. S22 (a and b) Cross-sectional and (c-i) top-view SEM images after Li deposition at 1 mAh cm^{-2} in the Ag-CS3 composite anode. (a, c, e, and h) Secondary electron (SE) mode and (b, d, f, and i) BSE-mode. (e and f) Enlarged SEM images of the yellow squares in (c) and (d), respectively, and (h and i) enlarged SEM images of the blue squares in (e) and (f), respectively.

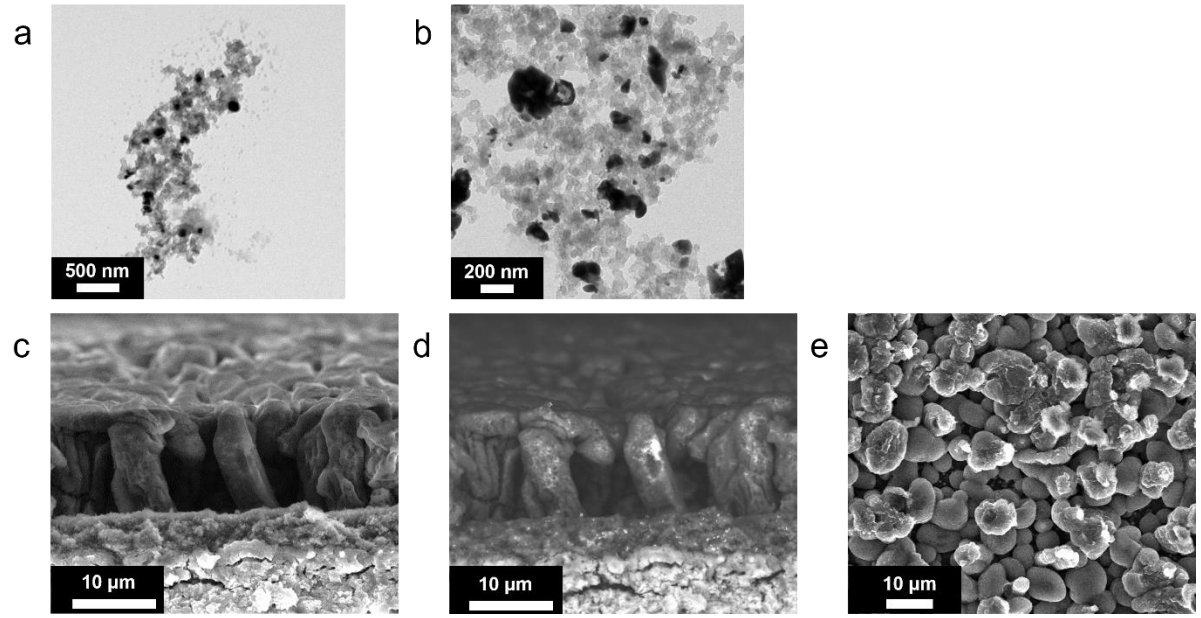

Fig. S23 (a and b) TEM images of Ag-decorated commercial carbon black (Ag-SC65). Cross-sectional SEM images obtained from (c) SE-mode and (d) BSE-mode, and (e) top-view SEM images of Ag-SC65 composite anodes with Li plated to a capacity of 3 mAh cm^{-2}.

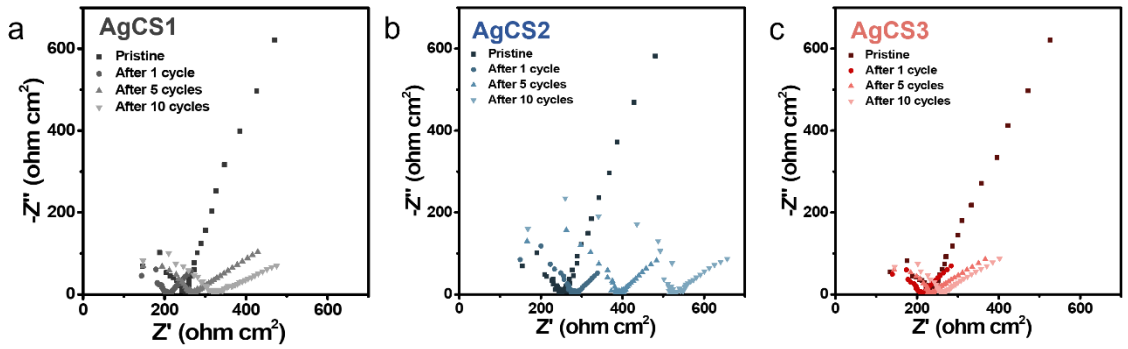

Fig. S24 Electrochemical impedance spectroscopic analysis (EIS) of (a) Ag-CS1, (b) Ag-CS2, and (c) Ag-CS3 in a pristine state before the test and after repeated Li plating and stripping.